0013-7227/02/$15.00/0
Printed in U.S.A.

Endocrinology 143(10):3813–3821

doi: 10.1210/en.2002-220121

Evaluation of Neuromedin U Actions in Energy Homeostasis and Pituitary Function

TINA R. IVANOV, CATHERINE B. LAWRENCE, PETER J. STANLEY, AND SIMON M. LUCKMAN

School of Biological Sciences, University of Manchester, Manchester, United Kingdom M13 9PT

The brain-gut peptide neuromedin U (NMU) has been identified recently as a physiological regulator of food intake. To further investigate the central role of NMU in energy homeostasis, we examined the distribution of NMU transcript and the effect of intracerebroventricular administration on several physiological parameters and on the pattern of c-Fos activation. Here we report that intracerebroventricular administration of NMU to 24-h fasted rats resulted in a decrease in subsequent food intake and body weight gain. NMU administration activated neurons in several brain regions implicated in the regulation of feeding behavior. Activated cells included catecholaminergic neurons of the arcuate nucleus and brain stem. Distribution studies revealed NMU expression in the caudal brain stem (nucleus of the solitary tract and inferior olive) and pituitary, with significant levels in the pars tuberalis. This contradicts earlier published observations. In obese (*fa/fa*) Zucker rats, decreases in NMU expression were detected in the nucleus of the solitary tract, pars tuberalis, and pars distalis, whereas in the fasted rat, a decrease in NMU transcript was detected in the pars distalis. These results confirm the effects of NMU on feeding and suggest additional roles for NMU in neuroendocrine function. (*Endocrinology* 143: 3813–3821, 2002)

NEUROMEDIN U (NMU) is a highly conserved molecule (1–3) originally purified from porcine spinal cord (4). First isolated in two molecular forms, NMU-8 constitutes the core active C terminus of NMU-25 (NMU-23 in rat), and both peptides potently stimulate smooth muscle contraction. NMU distribution studies using either an antibody to the peptide (5–9) or molecular probes (1, 10, 11) reveal relatively high levels of NMU expression in the pituitary (primarily, in corticotrophs of the anterior lobe), brain stem, gastrointestinal tract, thyroid gland, and ovary, suggesting additional biological roles for NMU beyond smooth muscle contraction.

NMU is involved in the central control of feeding (12). Intracerebroventricular (icv) administration of NMU results in a decrease in overnight food intake and time spent feeding, concomitant with transient increases in core body temperature, gross motor activity, and oxygen consumption (12–14). Central injection of anti-NMU IgG increases dark phase feeding, further suggesting that NMU is a potent endogenous anorexic peptide (13). Fasting rats for 48 h is reported to result in a significant decrease in NMU mRNA in the mediobasal hypothalamus ($-33 \pm 5\%$) relative to that in controls (12). In leptin-deficient *ob/ob* mice, levels of NMU mRNA in the suprachiasmatic nucleus (SCN) are reduced relative to those in lean controls (12).

NMU also affects the release of stress modulators, ACTH and corticosterone, from pituitary and adrenal glands, suggesting a role in the regulation of the hypothalamo-pituitary-adrenal axis (15). NMU has been linked to the thyroid axis, with reports that NMU content increases in the anterior pituitary after the administration of TRH (16). In addition, NMU increases arterial blood pressure (4) and modifies ion transport in the intestinal tract (17). The localization of NMU by RIAs to the nucleus accumbens and substantia nigra suggests an additional role for NMU in the modulation of dopaminergic action (6).

In situ analysis reveals a discrete pattern of NMU mRNA expression within the mediobasal aspect of the hypothalamus (lateral arcuate nucleus and median eminence) and caudal brain stem [nucleus of the solitary tract (NTS), area postrema, dorsal motor nucleus of the vagus nerve, and inferior olive] (12). Immunoreactive (-ir) cell bodies are reported exclusively in the arcuate nucleus rostrocaudally (8, 9), and NMU-ir fibers are widely distributed and are localized to the nucleus accumbens, hypothalamic regions (paraventricular nucleus and supraoptic nucleus), medial thalamus, and brain stem, with dense terminal fields primarily in the NTS and parabrachial nucleus (8, 9)

Biologically active NMUs are the endogenous ligands for two G protein-coupled receptors, FM-3 (hereafter referred to as NMU1R) and FM-4 (NMU2R) (3, 11–13, 18–21). NMU1R is expressed in numerous peripheral tissues, with little or no expression in the rat or human central nervous system (19, 21). In contrast, the highest levels of NMU2R transcript are located within the central nervous system and uterus. In the rat, NMU2R message has been detected by RT-PCR in the hypothalamus, spinal cord, and brain stem (18), and by *in situ* hybridization, transcript has been discretely localized in the paraventricular nucleus of the hypothalamus, along the third wall of the ventricle and the CA1 region of the hippocampus (12).

The aim of this study was to investigate further the central action of NMU on energy homeostasis. Having confirmed the acute effect of icv NMU administration on feeding and core body temperature, we determined, by c-Fos immunohistochemistry, the pattern of neuron activation after NMU administration. Key objectives were to reevaluate the distri-

Abbreviations: AUC, Area under the curve; DAB, diaminobenzidine; icv, intracerebroventricular; -ir, immunoreactivity, immunoreactive; NMU, neuromedin U; NTS, nucleus of the solitary tract; PB, phosphate buffer; SCN, suprachiasmatic nucleus; SSC, standard saline citrate; TH, tyrosine hydroxylase immunostaining.

bution of NMU mRNA in the brain and pituitary gland and to quantify changes in transcript levels in the 48-h fasted rat and in a chronic model of obesity, the Zucker rat.

Materials and Methods

Animals and surgery

Male Sprague Dawley rats (Charles River, Sandwich, UK), weighing 250–300 g, were housed at a constant ambient temperature of 21 ± 2 C on a 12-h light, 12-h dark cycle (lights on at 0800 h). Rat chow (Beekay International, Hull, UK) and tap water were provided *ad libitum* unless otherwise stated. All procedures conformed to the requirements of the UK Animals (Scientific Procedures) Act, 1986. For icv injection, rats were anesthetized with 2.5% halothane (AstraZeneca, Macclesfield, UK) and stereotaxically implanted with a guide cannula into the lateral ventricle (posterior, 0.8 mm; lateral, 1.5 mm from bregma) (22). The tip of the guide cannula was positioned 1 mm above the injection site (3.5 mm ventral from the surface of the skull). Core body temperature was monitored remotely in undisturbed animals by radiotransmitters (TA10TA-F40, Data Sciences, Minneapolis, MN) that were implanted into the peritoneum at the same time as cannulation. All animals were allowed to recover from surgery for a minimum of 5–7 d and then were housed individually. Intracerebroventricular injections were carried out in conscious unrestrained animals commencing 2 h after lights on (1000 h). For *in situ* hybridization experiments, male Sprague Dawley (48-h fasted, n = 6; fed, n = 6), and Zucker rats were used (lean *fa/+*, 280–350 g, n = 6; obese *fa/fa*, 415–480 g, n = 6; gifts from AstraZeneca).

Effect of NMU on food intake and body temperature

In the first experiment, vehicle (2 μl saline; n = 5) or rat NMU (4 nmol in 2 μl; n = 6; Bachem, Saffron Walden, UK) was injected into 24-h fasted rats. This dose was chosen after consultation of the literature and following our own preliminary experiments. For both free-feeding and fasted rats, dose-related physiological effects were obtained in response to 2 and 4 nmol NMU (results not shown). Immediately after injections, animals were presented with a preweighed amount of chow; food consumption was measured at 1, 2, 6, and 24 h, and body weight was determined at 6 and 24 h. In the second experiment, normally fed, satiated rats were injected icv with either vehicle (2 μl saline; n = 5) or rat NMU (4 nmol in 2 μl; n = 6). Food consumption and body weight were measured at 6 and 24 h. In both experiments core body temperature was monitored throughout the experimental period. All data are presented as the mean ± SEM. Food intake and body weight analyses were carried out using nonparametric Mann-Whitney *U* tests. Body temperatures were plotted as the mean change from the time of injection (time zero) and were analyzed by calculating the integrated temperature response for a defined period after injection [area under the curve (AUC); degrees centigrade per hour] for each animal by the trapezoidal method. Average AUC values were then determined for each treatment group.

Immunohistochemistry

Ninety minutes after icv administration of vehicle (n = 6) or 4 mol rat NMU (n = 6), deeply anesthetized rats were perfused transcardially with heparinized isotonic saline, followed by 4% paraformaldehyde in 0.1 M phosphate buffer (PB). Brains were removed, cryoprotected in 30% sucrose, and frozen at −80 C. Coronal sections (30 μm) were cut with a sledge microtome through the forebrain (−0.46 mm to −3.90 mm to bregma), and caudal brain stem (−13.44 mm to −15.46 mm to bregma), according to the atlas of Paxinos and Watson (22) and were collected in PB. To deactivate endogenous peroxidase activity, sections were incubated with 20% methanol, 0.2% Triton X-100, and 1.5% hydrogen peroxide for 20 min. Sections were washed in PB, blocked for 60 min in PB, 0.3% Triton X-100, and 2% normal sheep serum (blocking solution) and then incubated overnight at 4 C in blocking solution containing a 1:1000 dilution of rabbit polyclonal anti-c-Fos antibody (Calbiochem, Nottingham, UK). Sections were brought to room temperature, washed in PB, and incubated for 2 h with a peroxidase-labeled antirabbit IgG antibody (Vector Laboratories, Inc., Peterborough, UK) diluted 1:200 in blocking solution. Nickel-intensified diaminobenzidine [DAB; 0.1 M sodium acetate (pH 6.0), 2.5% nickel sulfate, 0.2% glucose, 0.04% ammonium chloride, 0.25% DAB, and ~30 U/ml glucose oxidase] was used as the chromogen in the peroxidase reaction to produce a purple-black nuclear c-Fos reaction product. The reaction was followed using a microscope and was terminated by sequential washes in acetate buffer and PB.

To identify catecholaminergic neurons, a set of c-Fos-labeled sections was further processed for tyrosine hydroxylase immunostaining (TH). After c-Fos immunodetection, sections were washed in PB and incubated overnight at 4 C in a 1:32,000 dilution of a mouse monoclonal anti-TH antibody (mAB318, Chemicon, Harrow, UK) in PB, 0.3% Triton X-100, and 2% normal horse serum. Sections were washed and incubated sequentially with a 1:200 dilution of biotinylated antimouse secondary antibody, then with a streptavidin-biotinylated horseradish peroxidase complex (Amersham Pharmacia Biotech, Little Chalfont, UK), each for 2 h. After PB washes, DAB (0.05% DAB and 0.01% H_2O_2 in PB) was used to produce a brown cytoplasmic TH-immunoreactive product. The reaction was monitored as before and was terminated in PB. Sections were mounted onto gelatin-coated microscope slides and coverslipped.

Catecholamine cell groups were identified from published descriptions. Cell bodies of tuberoinfundibular A12 dopaminergic neurons are located throughout the rostrocaudal aspect of the arcuate nucleus (23). At rostral levels of the hypothalamus, dopaminergic cell bodies of the A14 cell group are seen in the periventricular region surrounding the floor of the third ventricle and extending into the paraventricular nucleus. Perikarya of the A13 group are located in the dorsal hypothalamus, with a dense cluster of cells in the zona incerta. In the brain stem, the C1 cell group consists of a column of adrenergic cells in the ventrolateral medulla, which extends caudally into the A1 noradrenergic cell group (24, 25). Similarly, the C2 adrenergic cell group is situated dorsally in the NTS, rostral to the A2 noradrenergic cell group.

In situ hybridization

Quantitative *in situ* hybridization was performed using a single-stranded NMU antisense oligonucleotide identical in sequence to a previously described NMU probe (12). The oligonucleotide was end labeled with [^{35}S]deoxy-ATP (NEN Life Science Products, Hounslow, UK) and terminal deoxynucleotidyl transferase (Amersham Pharmacia Biotech) and was purified through a Sephadex G-50 column. Labeled NMU probe was successfully competed for by a 100-fold excess of cold probe oligonucleotide.

Coronal sections (15 μm) were cut from brain at the level of the arcuate nucleus (−1.78 mm to −3.70 mm to bregma) and caudal brain stem (−13.44 mm to −15.46 mm to bregma) (22) and through the pituitary gland. Before hybridization, sections were fixed for 30 min in cold 4% paraformaldehyde in 0.1 M PB (pH 7.4). Slides were rinsed twice in 0.1 M PBS (PB and 0.9% NaCl) and acetylated for 10 min in 0.25% acetic anhydride/0.1 M triethanolamine/0.9% NaCl. Sections were then taken through an increasing ethanol series, allowed to air-dry, and hybridized with 3×10^5 dpm/slide in buffer [10% dextran sulfate, 4× standard saline citrate (SSC; pH 7.0), 50% deionized formamide, 1× Denhardt's solution, and 0.4 mg/ml salmon testes DNA], overnight in a moist chamber at 37 C. After hybridization, slides were dipped in 1× SSC at room temperature and then washed three times for 30 min each time in 1× SSC at 55 C, followed by a room temperature wash for more than 60 min in 1× SSC. Slides were then briefly washed in 300 mM ammonium acetate and 70% ethanol and air-dried. Slides were exposed to K5 nuclear emulsion (Ilford, Knutsford, UK) for autoradiography, and quantitation of signal was performed using Northern Eclipse (Empix Imaging, Inc., Mississauga, Canada), a computer-based imaging system.

Results

Effect of NMU on food intake, change in body weight, and core body temperature

Intracerebroventricular injection of 4 nmol NMU caused a significant reduction in fast-induced refeeding at 1, 2, 6, and 24 h after injection compared with that in vehicle-treated animals ($P < 0.01$ for all time points; Fig. 1A). This was accompanied by a significant reduction in the change in body weight at 6 and 24 h ($P < 0.01$ for both time points; Fig. 1C). An increase in core body temperature was observed between

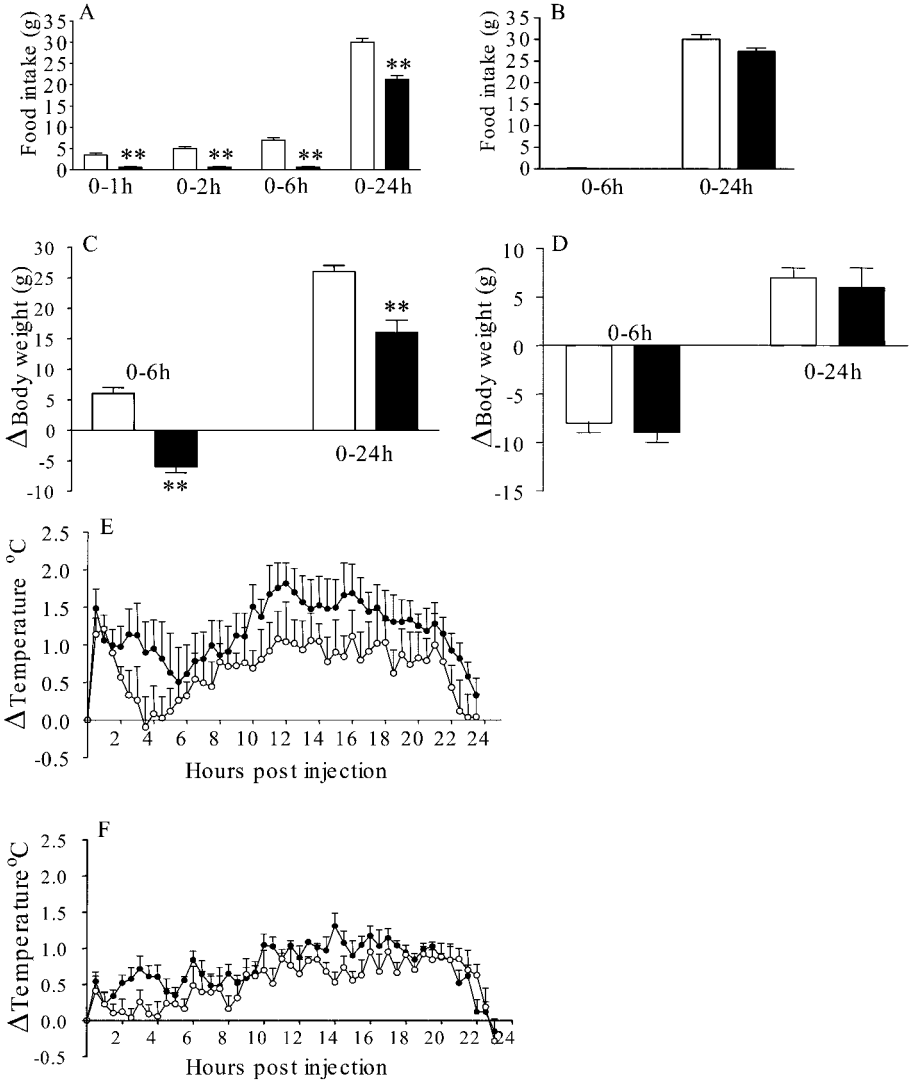

FIG. 1. Effects of 4 nmol NMU on food intake (A and B), change in body weight (C and D), and change in core body temperature (E and F) in 24-h fasted (A, C, and E) and satiated (B, D, and F) rats. The x-axis is hours after administration of rat NMU or vehicle (saline). Vehicle (□ or ○; n = 5) or 4 nmol NMU (■ or ●; n = 6) was administered icv at 1000 h. Data shown are the mean ± SEM. *Asterisks* indicate significant differences between NMU and vehicle groups. **, $P < 0.01$, by Mann-Whitney *U* test.

2 and 6 h, but failed to reach statistical significance (vehicle, 4.8 ± 1.2 C/h; NMU, 7.4 ± 1.6 C/h; $P = 0.24$, by unpaired *t* test on AUC; Fig. 1E). In satiated rats there was no significant difference in food intake (Fig. 1B) or change in body weight (Fig. 1D) over 6 and 24 h after NMU injection compared with vehicle-treated animals. Core body temperature was increased significantly in the NMU group between 2 and 4 h (vehicle, 2.2 ± 0.3 C/h; NMU, 3.2 ± 0.3 C/h; $P = 0.03$, by unpaired *t* test on AUC; Fig. 1F).

c-Fos induction

Compared with saline controls, 4 nmol NMU resulted in the induction of c-Fos-ir in several brain regions (Table 1 and Fig. 2). Within the hypothalamus, increased c-Fos-ir was detected in the paraventricular nucleus, arcuate nucleus, dorsomedial nucleus, and lateral hypothalamic area. NMU also induced c-Fos expression in the central nucleus of the amygdala, NTS, and ventrolateral medulla. An apparent change in c-Fos-ir noted in the ventral ependymal layer of the third ventricle was not statistically significant.

In the arcuate nucleus, cells expressing c-Fos were located in a continuum that started dorsomedially in the rostral arcuate to a ventrolateral pattern more caudally. This pattern is unlike that of neuronal types associated with feeding behavior, *e.g.* neuropeptide Y- and proopiomelanocortin-containing cells, but was similar to the distribution of TH-ir A12 dopaminergic cell bodies (23). Double immunolabeling revealed that 21 ± 3% of TH-ir neurons in the A12 were activated after NMU administration (saline, 1.3 ± 0.3%; $P = 0.002$; Table 2 and Fig. 3). Conversely, 26 ± 5% of all activated c-Fos cells in the arcuate were dopaminergic (saline, 7 ± 2%; $P = 0.009$). Little c-Fos and TH colocalization was observed for two other forebrain populations: the A13 dopaminergic neurons located in the zona incerta and the A14 dopaminergic neurons of the periventricular nucleus (Table 2). In the paraventricular nucleus, c-Fos ir cells were present in both parvicellular and magnocellular regions (Fig. 2).

In the caudal brain stem, c-Fos-ir cells were detected in the NTS and ventrolateral medulla, primarily at the level of the area postrema, with a decrease in number either more rostrally or more caudally. Colocalization studies demonstrated an activation of catecholaminergic neurons in the NTS and

TABLE 1. Number of c-Fos-ir cells in selected brain regions after icv administration of NMU

	No. of c-Fos-ir cells/section	
	Vehicle	4 nmol NMU
Amygdala (central nucleus)	36.0 ± 10	153.0 ± 23[a]
Supraoptic nucleus (h.)	14.0 ± 5	37.0 ± 10
Paraventricular nucleus (h.)	42.0 ± 10	194.0 ± 17[a]
Ventromedial nucleus (h.)	12.0 ± 5	23.0 ± 8
Dorsomedial nucleus (h.)	169.0 ± 25	270.0 ± 27[b]
Periventricular nucleus (h.)	17.0 ± 5	33.0 ± 11
Arcuate nucleus (h.)	11.0 ± 3	52.0 ± 7[a]
Dorsal ependyma (3rd v.)	78.0 ± 31	112.0 ± 29
Ventral ependyma (3rd v.)	45.0 ± 20	121.0 ± 28[c]
Lateral hypothalamic area	51.0 ± 10	98.0 ± 4[a]
Paraventricular thalamic area	95.0 ± 28	154.0 ± 31
NTS	13.0 ± 7	53.0 ± 7[d]
Area postrema	74.0 ± 7	75.0 ± 6
Ventrolateral medulla	3.0 ± 2	22.0 ± 2.0[a]

c-Fos-immunoreactive cells were counted 90 min after icv administration of 4 nmol NMU or vehicle. Significant differences are indicated between vehicle (n = 6) and NMU (n = 6) groups, by Mann-Whitney *U* test. h., Hypothalamic; NTS, nucleus of the solitary tract; v., ventricle. Values are the mean ± SEM.

[a] $P < 0.005$.
[b] $P < 0.05$.
[c] $P = 0.08$.
[d] $P < 0.01$.

ventrolateral medulla. In the NTS, 34 ± 4% of TH-ir cells expressed c-Fos after NMU administration compared with 3 ± 3% cells for saline controls ($P = 0.002$; Table 2 and Fig. 3). This expression overlap was most evident at the level of the area postrema, corresponding to the location of the A2 noradrenergic cell group. Few cells were double labeled in the NTS caudal to the area postrema. In the ventrolateral medulla, 27 ± 4% of TH-ir were immunoreactive for c-Fos after NMU administration compared with 0.2 ± 0.2% for saline controls ($P = 0.002$; Table 2 and Fig. 3). As with the NTS, double-labeled cells were observed primarily at the level of the area postrema corresponding to the A1/C1 overlap area. Rostral and caudal to the area postrema, the incidence of double-ir neurons in the ventrolateral medulla gradually decreased.

Expression of NMU

NMU transcript was detected in rat brain stem and pituitary gland. In caudal brain stem, significant and comparable levels were detected in the NTS (Fig. 4) and inferior olive (Table 3). Although not specifically analyzed, it appeared that gradients existed in the number of expressing cells (highest numbers at and rostral to area postrema) and the degree of expression (highest levels caudal to area postrema) in the NTS. Other brain stem regions expressing NMU included the dorsolateral surface of the brain stem (lateral to the spinal trigeminal nucleus) and, to a much lesser extent, the area postrema.

To determine whether NMU is regulated by changes in energy balance, NMU levels were compared in fasted and fed rats and in lean (*fa/+*) and obese (*fa/fa*) Zucker rats (Table 3). Within the NTS, small, nonsignificant decreases in NMU expression were observed in fasted rats relative to fed rats with respect to the level of NMU expression ($P = 0.13$) and the number of cells expressing NMU ($P = 0.052$). However, in the Zucker rat, a 81 ± 2.3% reduction in NMU expression was detected in the NTS of obese animals relative to lean. The number of cells expressing NMU did not differ between these two groups ($P = 0.61$). In the inferior olive, no differences were detected in the number of cells expressing NMU or the level of expression in either fasted or obese Zucker rats.

In the pituitary, a clustered pattern of NMU expression was observed in the pars tuberalis and pars distalis (Fig. 5). The signal in the pars tuberalis was seen clearly in coronal sections through the tuberoinfundibulum, abutting the ventral surface of the median eminence. Silver grains were not at a single plane of focus suggesting the organization of expressing cells into tubes or follicles. In the pars distalis, clusters of cells expressed NMU at relatively high levels against a background of low expressing cells. NMU transcript was also detected throughout the pars intermedia, but was absent in the pars nervosa and hypothalamic regions, including the median eminence and arcuate nucleus.

Due to the small size and dense packing of cells in the pars tuberalis, pars distalis, and pars intermedia, a measurement of the number of grains per cell and the number of NMU-expressing cells was problematic, and a measurement of grain density was made instead (Table 4). In the pars tuberalis, no significant difference was observed in NMU expression between fed and fasted rats. A significant reduction in expression (−72 ± 4.4%), however, was detected in obese Zucker rats relative to lean animals. In the pars distalis, a decrease in grain density was observed for both fasted rats (−68 ± 6.6%) and obese Zucker rats (−57 ± 13.1%). No differences in NMU expression were observed for either fasted or obese Zucker rats in the pars intermedia.

Discussion

Intracerebroventricular administration of 4 nmol NMU to 24-h fasted rats resulted in a significant decrease in subsequent refeeding, confirming the potent action of this peptide as an anorexigen (12–14). Concomitant with the decrease in food intake are increases in core body temperature and oxygen consumption, indicating increased energy expenditure (12, 14). These factors combine to reduce body weight gain over the acute phase. In the present experiments involving fasted rats, NMU administration resulted in a trend toward an increase in core body temperature, although this did not quite reach statistical significance, probably due to large variations in core body temperature in fasted animals. However, we have shown that NMU administered to satiated rats increased core body temperature in the absence of feeding behavior, suggesting that the feeding response and the effects on energy expenditure of NMU can be dissociated. The increase in energy expenditure may reflect some of the other consequences of central NMU administration, which include increased locomotor activity and grooming, or adaptive thermogenesis (12, 14, 26).

The distribution of NMU in the brain and pituitary suggests that it may have a variety of functions (8, 9, 12) and makes determination of the mechanism of NMU action on food intake and body weight complex. Howard and colleagues (12) have reported a change in the expression of

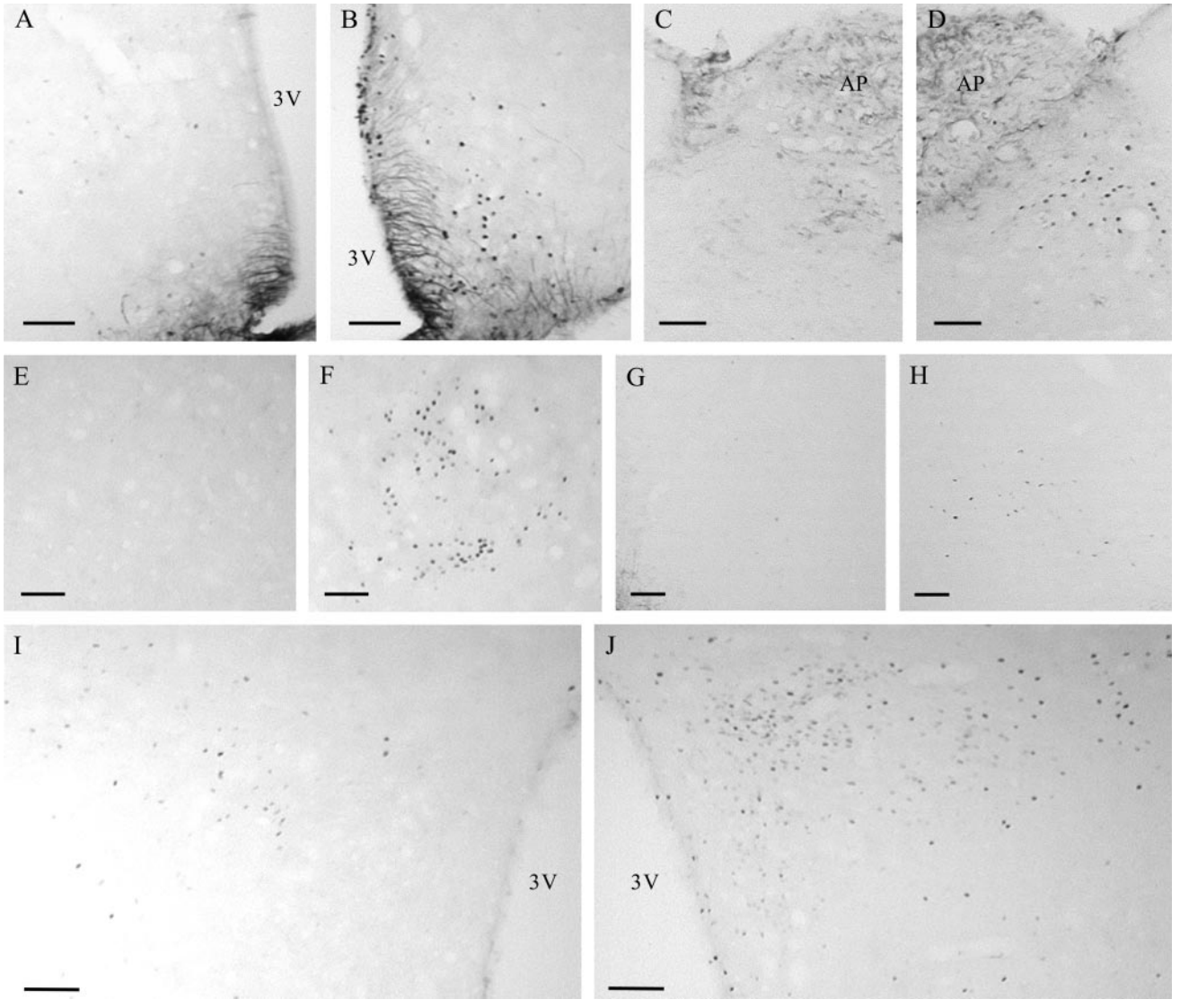

FIG. 2. Representative photomicrographs of c-Fos-ir cell nuclei in selected brain regions after the administration of either vehicle (A, C, E, G, and I) or 4 nmol NMU (B, D, F, H, and J). Rats were killed 90 min post injection, sections were cut, and immunocytochemistry was performed using a c-Fos antibody. Brain regions shown include the arcuate nucleus (A and B), the NTS (C and D), the central nucleus of the amygdala (E and F), the ventrolateral medulla (G and H), and the hypothalamic paraventricular nucleus (I and J). 3V, Third ventricle; AP, area postrema. *Scale bar*, 200 μm (for all panels).

TABLE 2. Activation of tyrosine hydroxylase-ir cells after NMU administration

	% c-Fos cells expressing TH		% TH cells expressing c-Fos	
	Vehicle	4 nmol NMU	Vehicle	4 nmol NMU
Arcuate nucleus (h.)	7.0 ± 2	26.0 ± 5[a]	1.3 ± 0.3	21.0 ± 3[b]
Periventricular nucleus (h.)	5.0 ± 1	10.0 ± 3	3.0 ± 1	3.0 ± 1
Zona incerta	3.0 ± 1	5.0 ± 1	1.2 ± 0.4	2.3 ± 1
NTS	2.0 ± 1	11.0 ± 3[b]	3.0 ± 3	34.0 ± 4[b]
Ventrolateral medulla	0.2 ± 0.2	23.0 ± 5[b]	0.2 ± 0.17	27.0 ± 4[b]

c-Fos- and tyrosine hydroxylase-ir cells were counted 90 min after icv administration of 4 nmol NMU or vehicle. Significant differences are indicated between vehicle (n = 6) and NMU (n = 6) groups, by Mann-Whitney *U* test. h., Hypothalamic; NTS, nucleus of the solitary tract. Values are the mean ± SEM.

[a] $P < 0.01$.

[b] $P < 0.005$.

NMU mRNA in ventromedial hypothalamic regions in what they term the lateral arcuate nucleus and median eminence of fasted rats. This coupled with the lack of conditioned taste aversion after central administration of the peptide (12) suggested that NMU is an endogenous regulator of food intake. However, careful examination of emulsion-dipped slides in

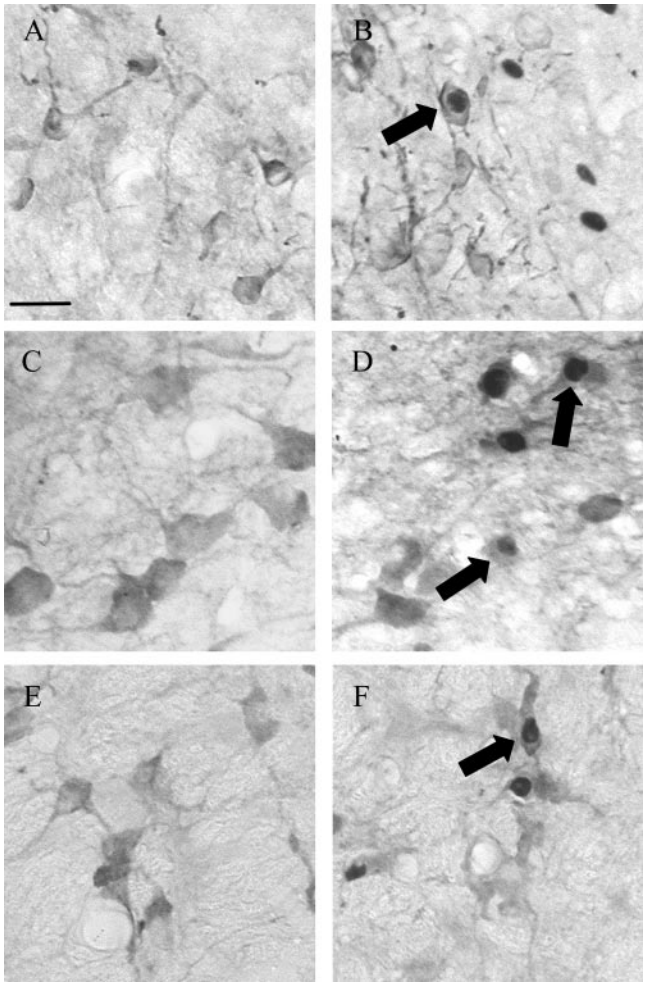

FIG. 3. Activation of tyrosine hydroxylase neurons after the administration of NMU. Slides were processed as described in Fig. 2, except that sections were sequentially immunoreacted with antibodies to c-Fos and tyrosine hydroxylase. A and B, Arcuate nucleus; C and D, NTS; E and F, ventrolateral medulla. A, C, and E, Vehicle-injected rats; , D, and F, 4 nmol NMU-injected rats B. *Arrows* indicate activated tyrosine hydroxylase neurons. *Scale bar*, 50 μm (for all panels).

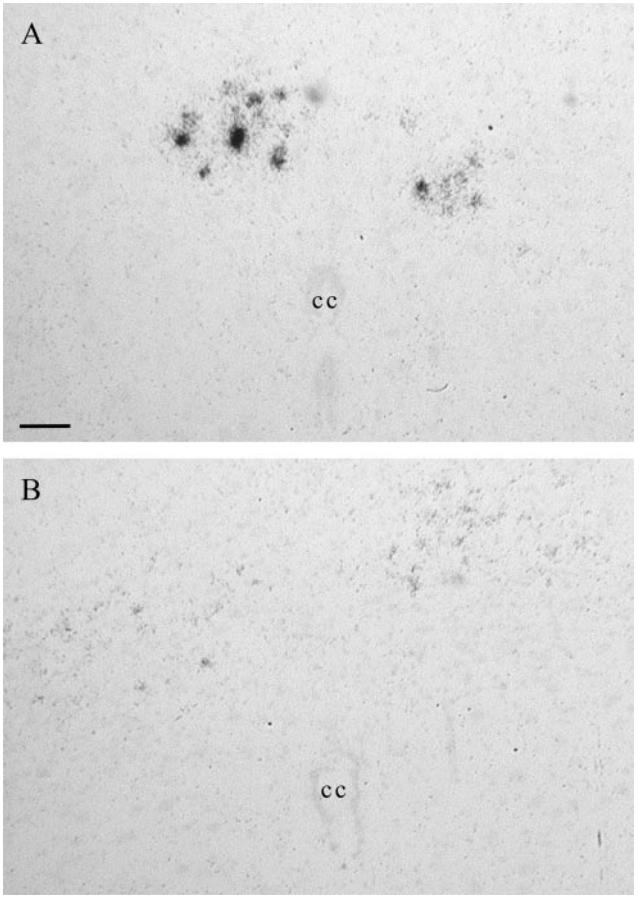

FIG. 4. Expression of NMU in caudal brain stem NTS in lean (*fa/+*) and obese (*fa/fa*) Zucker rats by *in situ* hybridization. Sections were hybridized with a previously described NMU ^{35}S-labeled oligonucleotide probe, washed, and dipped in nuclear emulsion. Slides were exposed for 8 wk. After development of signal, sections were lightly counterstained with cresyl violet. A, Lean (*fa/+*); B, obese (*fa/fa*). cc, Central canal. *Scale bar*, 200 μm.

our experiments revealed that NMU message is present not in either the arcuate nucleus or the median eminence, but, rather, in the pituitary pars tuberalis, a highly vascularized, multicellular tube of cells that surrounds the hypophyseal stalk and extends along the ventral surface of the median eminence (27, 28). The detection of NMU in the pars tuberalis is also seemingly at odds with immunocytochemistry that describes the presence of NMU in the arcuate nucleus (8, 9). However, although not discussed in the text of these previous papers, immunoreactive material is clearly visible on the ventral surface of the hypothalamus corresponding to the location of the pars tuberalis (8). Furthermore, another study that used a different antibody (29) failed to detect NMU-ir cell bodies in the arcuate nucleus. We have now confirmed our pattern of NMU mRNA expression with a second oligonucleotide probe to a different portion of the NMU transcript and with a ^{33}P-labeled riboprobe (data not shown), suggesting that localization of NMU in the pars tuberalis and not in the arcuate nucleus is correct.

Here we demonstrate the regulation of NMU expression in both the pituitary and a separate brain region (the NTS) in two models of energy imbalance, the fasted rat and the Zucker rat. In the obese Zucker rat, which lacks a functional leptin receptor and is hyperphagic, NMU expression was significantly reduced in the brain stem NTS. Such a reduction in the expression of putative anorexic peptides in Zucker rats has been reported widely (30–32). The selectivity of this adaptation is exemplified by the lack of change in another population of the brain stem, NMU-expressing cells in the inferior olive. It is possible that the brain stem population of NMU-expressing cells is more important in mediating appetite effects. The NTS is involved in a number of autonomic and neuroendocrine functions. After the ingestion of a satiating meal, gastric distension and nutrients in the gut signal to the NTS, and this information is relayed to other brain stem and forebrain regions involved in the control of feeding (33).

The change in NMU expression in the pituitary may be secondary to endocrine adaptation in states of energy imbalance. Both fasted and Zucker rats show obvious changes in endocrine function, including decreased levels of GH and

TABLE 3. Expression of NMU in caudal brainstem

	No. of silver grains/cell		No. of expressing cells/section	
	Fed	48 h Fast	Fed	48 h Fast
NTS	92 ± 9	73 ± 8	72 ± 3	53 ± 5[a]
Inferior olive	92 ± 8	95 ± 10	49 ± 5	49 ± 4
	Lean (*fa*/+)	Obese (*fa*/*fa*)	Lean (*fa*/+)	Obese (*fa*/*fa*)
NTS	223 ± 50	43 ± 5[b]	26 ± 5	22 ± 5
Inferior olive	59 ± 9	61 ± 7	18 ± 2	17 ± 2

Significant differences are indicated between fed (n = 6) and 48-h fasted (n = 6) Sprague-Dawley rats and between lean (n = 6) and obese (n = 6) Zucker rats, by Mann-Whitney *U* test. NTS, Nucleus of the solitary tract. Values are the mean ± SEM.

[a] $P = 0.052$.

[b] $P < 0.005$.

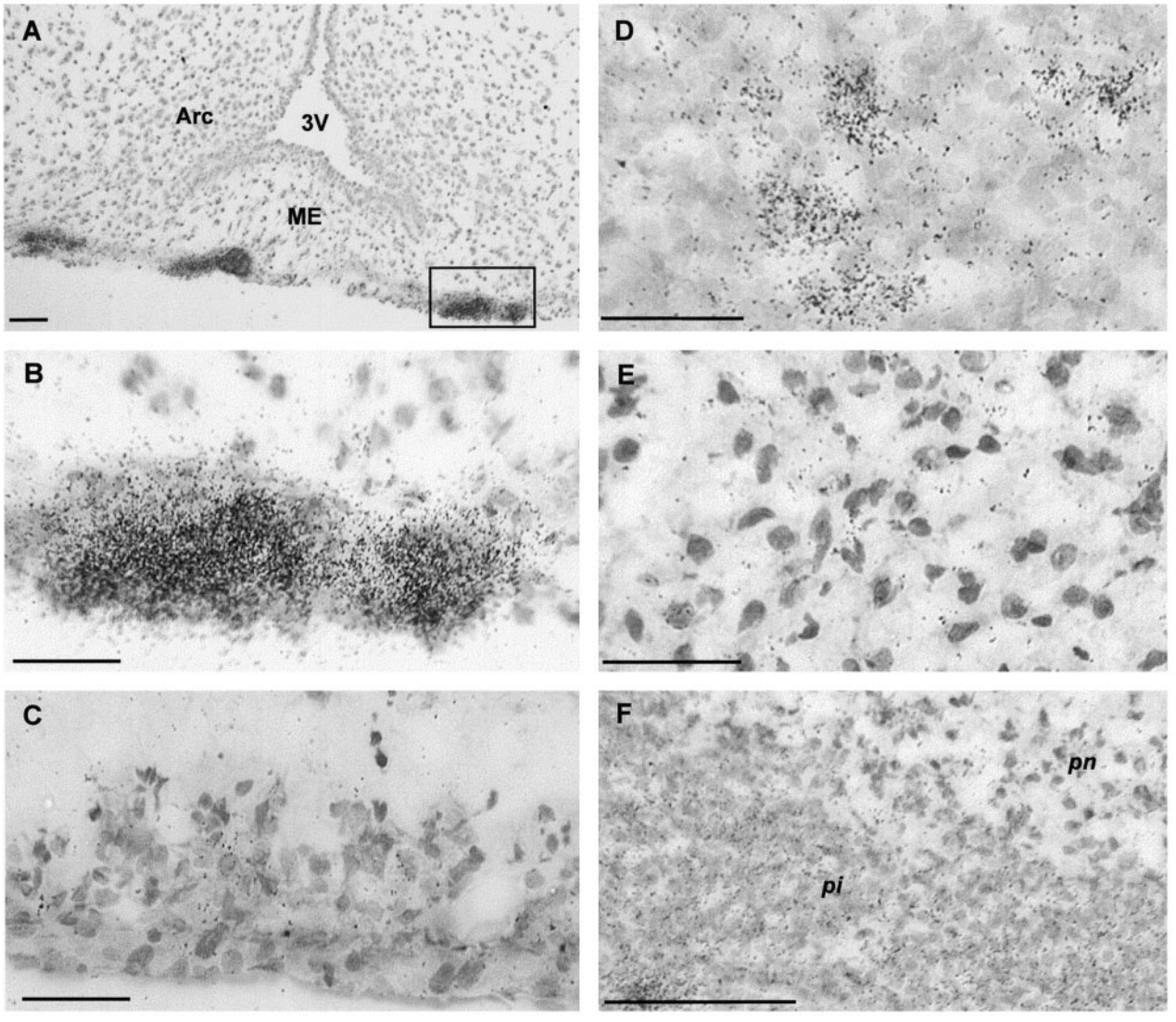

FIG. 5. Detection of NMU mRNA in rat pituitary gland. Coronal sections through hypothalamus and pituitary gland were processed as described in Fig. 4. A–C, Coronal hypothalamic sections, showing the pars tuberalis. B, Higher magnification of the *boxed area* in A. C, Representative of a pars tuberalis section hybridized with a 100-fold excess of cold NMU oligonucleotide. D–F, Pituitary sections showing pars distalis, pars nervosa, and pars intermedia, respectively. Slides were exposed for 4 wk. 3V, Third ventricle; Arc, arcuate nucleus; ME, median eminence; pi, pars intermedia; pn, pars nervosa. *Scale bar*, 100 μm (except 200 μm in A).

thyroid hormone (34). A photoperiodic function has been assigned to the pars tuberalis in some species, in that melatonin acts here to modulate the seasonal changes in pituitary PRL output (28). Interestingly, NMU is expressed in all regions of the rat pituitary except the pars nervosa, and its expression was down-regulated in both the pars tuberalis and the pars distalis of obese Zucker rats. Previous pituitary immunocytochemistry has localized NMU expression in a

TABLE 4. Expression of NMU in the pituitary gland

	No. of silver grains/100 μm^2	
	Fed	48-h fasted
Pars tuberalis	30.0 ± 10.0	23.0 ± 4.0
Pars distalis	31.0 ± 1.0	10.0 ± 2.0[a]
Pars intermedia	15.0 ± 5.0	15.0 ± 2.0
	Lean (*fa*/+)	Obese (*fa*/*fa*)
Pars tuberalis	66.0 ± 20.0	15.0 ± 2.0[a]
Pars distalis	24.0 ± 3.0	11.0 ± 3.0[b]
Pars intermedia	11.0 ± 3.0	8.0 ± 2.0

Significant differences are indicated between fed (n = 6) and 48-h fasted (n = 6) and between lean (n = 6) and obese (n = 6) Zucker rats, by Mann-Whitney *U* test. Values are the mean ± SEM.

[a] $P < 0.01$.

[b] $P < 0.05$.

subset of pars distalis cells, including corticotropes and thyrotropes (5, 6, 8, 9). A decrease in pars distalis NMU expression was also noted in rats fasted for 48 h. The lack of modulation in the adjacent pars intermedia suggests selectivity in the response.

NMU administration induced prominent c-Fos expression in central areas, including those involved in the control of feeding behavior (paraventricular nucleus, arcuate nucleus, caudal brain stem, and central nucleus of the amygdala). The robust induction of c-Fos in the paraventricular nucleus may relate to the reported presence of dense NMU-ir fibers (8) and the NMU2R receptor message in this hypothalamic nucleus (12). This activation might include parvicellular neurons containing CRH, as these neurons are important in feeding and have recently been implicated in the locomotor activity induced by NMU (26). Interestingly, both NMU-ir fibers (8) and NMU2R mRNA are also found in cells of the ventral ependyma lining the third ventricle (12). Although icv injections commonly induce some c-Fos expression in the ependyma, in the present experiments more c-Fos immunoreactivity was detected in the ventral ependyma of the third ventricle of NMU-treated rats compared with vehicle-treated rats. Although this did not quite reach statistical significance, it warrants further investigation, because pituitary control of hypothalamic function has been previously suggested (28).

A prominent c-Fos induction was also observed in the arcuate nucleus, which is an important site for the integration of information concerning body weight regulation, notably by leptin-sensitive neuropeptide Y and proopiomelanocortin neurons (35). However, a significant population of the neurons activated in the dorsomedial and ventrolateral arcuate nucleus colocalized with tyrosine hydroxylase. Dorsomedial TH-ir neurons predominantly innervate the mid portion of the median eminence and are believed to inhibit PRL release from pituitary pars distalis lactotropes by the release of dopamine. Ventrolateral TH-ir neurons innervate lateral aspects of the median eminence, but the function of these cells is unknown, as they lack dihydroxyphenylalanine decarboxylase and do not synthesize dopamine (36). It is possible that if NMU from the pars tuberalis is capable of releasing PRL from the pituitary, the induction of c-Fos in dopaminergic neurons of the arcuate nucleus is secondary to negative feedback by this hormone (37). A link between NMU and dopaminergic function in other parts of the brain has been made previously (6). Alternatively, the c-Fos-ir noted here in the hypothalamus and amygdala may result indirectly from the activation of afferent cells. Catecholaminergic neurons in the NTS and ventrolateral medulla project to both the hypothalamus and central nucleus of the amygdala (38). By double immunocytochemistry, NMU was shown to induce c-Fos expression in 34% and 27% of TH-ir neurons in the NTS and ventrolateral medulla, respectively. For comparison, peripheral injection of another anorexic factor, cholecystokinin, which also activates the paraventricular nucleus and amygdala, results in c-Fos expression in 43% of catecholaminergic NTS neurons and in 46% of catecholaminergic ventrolateral medulla neurons (39).

Clearly, NMU is a potent anorexic peptide when administered centrally. The lack of a conditioned taste aversion by the same stimulus also suggests that it is of physiological relevance (12). Here we demonstrate that chronic imbalance of energy homeostasis, as seen in the obese Zucker rat, elicits regulation of NMU mRNA expression similar to that in fasted animals. The relative importance of different populations of NMU-expressing cells on food intake remains to be determined, although the population in the brain stem NTS may be well placed to mediate satiety signaling. We also demonstrate a response of NMU cells in certain regions of the pituitary, which may result from adaptation of endocrine systems to energy imbalance. Interestingly, in the mouse, NMU transcript is detected in the SCN of the hypothalamus (12), the site of the mammalian master circadian pacemaker. In the homozygote *ob*/*ob* mouse, which lacks circulating leptin, there is a reduction in the expression of NMU mRNA in the SCN (12). Although we did not detect NMU in the SCN of rats, regulation in the mouse SCN resembles our reported decrease in NMU mRNA in the obese Zucker's pars tuberalis, another structure noted for its biological time keeping.

Acknowledgments

Received January 31, 2002. Accepted June 11, 2002.

Address all correspondence and requests for reprints to: Dr. Simon M. Luckman, University of Manchester School of Biological Sciences, 1.124 Stopford Building, Oxford Road, Manchester, United Kingdom M13 9PT. E-mail: simon.luckman@man.ac.uk.

This work was supported by AstraZeneca Plc. and the Biotechnology and Biological Sciences Research Council.

References

1. **Lo G, Legon S, Austin C, Wallis S, Wang Z, Bloom SR** 1992 Characterization of complementary DNA encoding the rat neuromedin U precursor. Mol Endocrinol 6:1538–1544
2. **Maderdrut JL, Lazar G, Kozicz T, Merchenthaler I** 1996 Distribution of neuromedin U-like immunoreactivity in the central nervous system of *Rana esculenta*. J Comp Neurol 369:438–450
3. **Hedrick JA, Morse K, Shan L, Qiao X, Pang L, Wang S, Laz T, Gustafson EL, Bayne M, Monsma Jr FJ** 2000 Identification of a human gastrointestinal tract and immune system receptor for the peptide neuromedin U. Mol Pharmacol 58:870–875
4. **Minamino N, Kangawa K, Matsuo H** 1985 Neuromedin U-8 and U-25: novel uterus stimulating and hypertensive peptides identified in porcine spinal cord. Biochem Biophys Res Commun 130:1078–1085
5. **Cimini V, Van Noorden S, Timson CM, Polak JM** 1993 Modulation of galanin and neuromedin U-like immunoreactivity in rat corticotropes after alteration in endocrine status. Cell Tissue Res 272:137–146
6. **Domin J, Ghatei MA, Chohan P, Bloom SR** 1987 Neuromedin U: a study of its distribution in the rat. Peptides 8:779–784
7. **Domin J, Al-Madani AM, Desperbasques M, Bishop AE, Polak JM, Bloom SR** 1990 Neuromedin U-like immunoreactivity in the thyroid gland. Cell Tissue Res 260:131–135
8. **Ballesta J, Carlei F, Bishop AE, Steel JH, Gibson SJ, Fahey M, Hennessey R, Domin J, Bloom SR, Polak JM** 1988 Occurrence and developmental pattern

of neuromedin U-immunoreactive nerves in the gastrointestinal tract and brain of the rat. Neuroscience 25:797–816

9. **Steel JH, Van Noorden S, Ballesta J, Gibson SJ, Ghatei MA, Burrin J, Leonhardt U, Domin J, Bloom SR, Polak JM** 1988 Localization of 7B2, neuromedin B, and neuromedin U in specific cell types of rat, mouse and human pituitary, in rat hypothalamus and in 30 human pituitary and extrapituitary tumors. Endocrinology 122:270–282
10. **Austin C, Oka M, Nandha KA, Legon S, Khandan-Nia N, Lo G, Bloom SR** 1994 Distribution and developmental pattern of neuromedin U expression in the rat gastrointestinal tract. J Mol Endocrinol 12:257–263
11. **Fujii R, Hosoya M, Fukusumi S, Kawamata Y, Habata Y, Hinuma S, Onda H, Nishimura O, Fujino M** 2000 Identification of neuromedin U as the cognate ligand of the orphan G protein-coupled receptor FM-3. J Biol Chem 275:21068–21074
12. **Howard AD, Wang R, Pong S-S, Mellin TN, Strack A, Guan X-M, Zeng Z, Williams DL, Feighner SD, Nunes CN, Murphy B, Stair JN, Yu H, Jiang Q, Clements MK, Tan CP, McKee KK, Hreniuk DL, McDonald TP, Lynch KR, Evans JF, Austin CP, Caskey CT, Van der Ploeg LHT, Liu Q** 2000 Identification of receptors for neuromedin U and its role in feeding. Nature 406:70–74
13. **Kojima M, Haruno R, Nakazato M, Date Y, Murakami N, Hanada R, Matsuo H, Kangawa K** 2000 Purification and identification of neuromedin U as an endogenous ligand for an orphan receptor GPR66 (FM3). Biochem Biophys Res Commun 276:435–438
14. **Nakazato M, Hanada R, Murakami N, Date Y, Mondal MS, Kojima M, Yoshimatsu H, Kangawa K, Matsukura S** 2000 Central effects of neuromedin U in the regulation of homeostasis. Biochem Biophys Res Commun 277:191–194
15. **Malendowicz LK** 1998 Role of neuromedins in the regulation of adrenocortical function. Horm Metab Res 30:374–384
16. **Domin J, Steel JH, Adolphus N, Burrin JM, Leonhardt U, Polak JM, Bloom SR** 1989 The anterior pituitary content of neuromedin U-like immunoreactivity is altered by thyrotrophin-releasing hormone and thyroid hormone status in the rat. J Endocrinol 122:471–476
17. **Sumi S, Inoue K, Kogire M, Doi R, Takaori K, Suzuki T, Tobe T** 1987 Effect of synthetic neuromedin U-8 and U-25 novel peptides identified in porcine spinal cord on splanchnic circulation in dogs. Life Sci 41:1585–1590
18. **Hosoya M, Moriya T, Kawamata Y, Ohkubo S, Fujii R, Matsui H, Shintani Y, Fukusumi S, Habata Y, Hinuma S, Onda H, Nishimura O, Fujino M** 2000 Identification and functional characterization of a novel subtype of neuromedin U receptor. J Biol Chem 275:29528–29532
19. **Raddatz R, Wilson AE, Artymyshyn R, Bonini JA, Borowsky B, Boteju LW, Zhou S, Kouranova EV, Nagorny R, Guevarra MS, Dai M, Lerman GS, Vaysse PJ, Branchek TA, Gerald C, Forray C, Adham N** 2000 Identification and characterization of two neuromedin U receptors differentially expressed in peripheral tissues and the central nervous system. J Biol Chem 275:32452–32459
20. **Shan L, Qiao X, Crona JH, Behan J, Wang S, Laz T, Bayne M, Gustafson EL, Monsma Jr FJ, Hedrick JA** 2000 Identification of novel neuromedin U receptor subtype expressed in the central nervous system. J Biol Chem 275:39482–39486
21. **Szekeres PG, Muir AI, Spinage LD, Miller JE, Butler SI, Smith A, Rennie GI, Murdock PR, Fitzgerald LR, Wu H, McMillan LJ, Guerrera S, Vawter L, Elshourbagy NA, Mooney JL, Bergsma DJ, Wilson S, Chambers JK** 2000 Neuromedin U is a potent agonist at the orphan G protein-coupled receptor FM3. J Biol Chem 275:20247–20250
22. **Paxinos G, Watson C** 1986 The rat brain in stereotaxic coordinates. London: Academic Press
23. **Okamura H, Kitakama K, Nagatsu I, Geffard M** 1988 Comparative topography of dopamine- and tyrosine hydroxylase-immunoreactive neurons in the rat arcuate nucleus. Neurosci Lett 95:347–353
24. **Kalia M, Fuxe K, Goldstein M** 1985 Rat medulla oblongata. II. Dopaminergic, noradrenergic (A1 and A2) and adrenergic neurons, nerve fibers, and presumptive terminal processes. J Comp Neurol 233:308–332
25. **Kalia M, Fuxe K, Goldstein M** 1985 Rat medulla oblongata. III. Adrenergic (C1 and C2) neurons, nerve fibers and presumptive terminal processes. J Comp Neurol 233:333–349
26. **Hanada R, Nakazato M, Murakami N, Sakihara S, Yoshimatsu H, Toshinai K, Hanada T, Suda T, Kangawa K, Matsukura S, Sakata T** 2001 A role for neuromedin U in stress response. Biochem Biophys Res Commun 289:225–228
27. **Wittkowski W, Bockmann J, Kreutz MR, Bockers TM** 1999 Cell and molecular biology of the pars tuberalis of the pituitary. Int Rev Cytol 185:157–184
28. **Morgan PJ, Williams LM** 1996 The pars tuberalis of the pituitary: a gateway for neuroendocrine output. Rev Reprod 1:153–161
29. **Honzawa M, Sudoh T, Minamino N, Tohyama M, Matsuo H** 1987 Topographic localization of neuromedin U-like structures in the rat brain: an immunohistochemical study. Neuroscience 23:1103–1122
30. **Richard D, Rivest R, Naimi N, Timofeeva E, Rivest S** 1996 Expression of corticotropin-releasing factor and its receptors in the brain of lean and obese Zucker rats. Endocrinology 137:4786–4795
31. **Kristensen P, Judge ME, Thim L, Ribel U, Christjansen KN, Wulff BS, Clausen JT, Jensen PB, Madsen OD, Vrang N, Larsen PJ, Hastrup S** 1998 Hypothalamic CART is a new anorectic peptide regulated by leptin. Nature 393:72–76
32. **Kim EM, O'Hara E, Grace MK, Welch CC, Billington CJ, Levine AS** 2000 ARC POMC mRNA and PVN α-MSH are lower in obese relative to lean Zucker rats. Brain Res 862:11–16
33. **Rinaman L, Baker EA, Hoffman GE, Stricker EM, Verbalis JG** 1998 Medullary c-Fos activation in rats after ingestion of a satiating meal. Am J Physiol 275:R262–R268
34. **Elmquist JK, Maratos-Flier E, Saper CB, Flier JS** 1998 Unraveling the central nervous system pathways underlying responses to leptin. Nat Neurosci 1:445–450
35. **Baskin DG, Lattemann DF, Seeley RJ, Woods SC, Porte Jr D, Schwartz MW** 1999 Insulin and leptin: dual adiposity signals to the brain for the regulation of food intake and body weight. Brain Res 848:114–123
36. **Meister B, Hokfelt T, Vale WW, Sawchenko PE, Swanson L, Goldstein M** 1986 Coexistence of tyrosine hydroxylase and growth hormone-releasing factor in a subpopulation of tubero-infundibular neurons of the rat. Neuroendocrinology 42:237–247
37. **Demaria JE, Nagy GM, Freeman ME** 2000 Immunoneutralization of prolactin prevents stimulatory feedback of prolactin on hypothalamic neuroendocrine dopaminergic neurons. Endocrine 12:333–337
38. **Petrov T, Krukoff TL, Jhamandas JH** 1993 Branching projections of catecholaminergic brainstem neurons to the paraventricular hypothalamic nucleus and the central nucleus of the amygdala in the rat. Brain Res 609:81–92
39. **Luckman S** 1992 Fos-like immunoreactivity in the brainstem of the rat following peripheral administration of cholecystokinin. J Neuroendocrinol 4:149–152